American Journal of Transplantation 2009; 9: 517–526
Wiley Periodicals Inc.

doi: 10.1111/j.1600-6143.2008.02512.x

Renal Allografts with IF/TA Display Distinct Expression Profiles of Metzincins and Related Genes

S. Rödder[a,*], A. Scherer[b], F. Raulf[c], C. C. Berthier[d], A. Hertig[e,f], L. Couzi[g], A. Durrbach[h], E. Rondeau[e,f] and H.-P. Marti[a,f]

[a] *Department of Nephrology and Hypertension, Inselspital Bern, University Hospital, University Bern, Switzerland*
[b] *Spheromics, Kontiolahti, Finland*
[c] *Novartis Institutes for BioMedical Research, Basel, Switzerland*
[d] *University of Michigan, Department of Internal Medicine – Nephrology, Ann Arbor, MI*
[e] *Department of Nephrology and Kidney Transplantation, Hôpital Tenon, Paris, France*
[f] *INSERM, Unite 702, Hôpital Tenon, Paris, France*
[g] *Nephrology Department, Hôpital Pellegrin-Tripode, C.H.U. Bordeaux, France*
[h] *Nephrology Department, IFRNT, Le Kremlin Bicetre, Université Paris Sud, France*
* *Corresponding author: Silke Rödder, silke.roedder@dkf.unibe.ch*

Chronic renal allograft injury is often reflected by interstitial fibrosis (IF) and tubular atrophy (TA) without evidence of specific etiology. In most instances, IF/TA remains an irreversible disorder, representing a major cause of long-term allograft loss. As members of the protease family metzincins and functionally related genes are involved in fibrotic and sclerotic processes of the extracellular matrix (ECM), we hypothesized their deregulation in IF/TA. Gene expression and protein level analyses using allograft biopsies with and without Banff'05 classified IF/TA illustrated their deregulation. Expression profiles of these genes differentiated IF/TA from Banff'05 classified Normal biopsies in three independent microarray studies and demonstrated histological progression of IF/TA I to III. Significant upregulation of matrix metalloprotease-7 (MMP-7) and thrombospondin-2 (THBS-2) in IF/TA biopsies and sera was revealed in two independent patient sets. Furthermore, elevated THBS-2, osteopontin (SPP1) and β-catenin may play regulatory roles on MMP. Our findings further suggest that deregulated ECM remodeling and possibly epithelial to mesenchymal transition (EMT) are implicated in IF/TA of kidney transplants, and that metzincins and related genes play an important role in these processes. Profiling of these genes may be used to complement IF/TA diagnosis and to disclose IF/TA progression in kidney transplant recipients.

Key words: Chronic allograft injury, extracellular matrix, IF/TA, matrix metalloproteases, MMP-7, transcriptomics

Received 03 June 2008, revised 10 October 2008 and accepted for publication 08 November 2008

Introduction

A leading cause of chronic renal allograft injury (CAI) remains progressive deterioration of kidney function, reflected by interstitial fibrosis and tubular atrophy without evidence of specific etiology (IF/TA), often accompanied by arterial hypertension and calcineurin inhibitor (CNI) toxicity (1). Biopsy-based diagnosis of CAI is often delayed since clinical indicators manifest themselves typically after pathohistological alterations have been established (2–5). To date, there is no specific and effective treatment to reverse established IF/TA.

Evidence exists, that IF/TA arises at an early stage during CAI progression (4). Therefore, identification of fibrogenic factors may complement diagnosis prior to the occurrence of histological damage and lead to indicative parameters of IF/TA progression and potential therapeutic targets.

Fibrosis is characterized by accumulation of ECM proteins including deregulation of ECM remodeling (6,7). ECM remodeling is regulated by the superfamily of metzincins (METS), zinc-dependent, metalloproteases (8,9). These enzymes can be subdivided into a disintegrin and metalloprotease domain (ADAM), a disintegrin and metalloprotease domain with thrombospondin-motif (ADAMTS), serralysins, papalysins and matrix metalloproteases (MMP) (8). The latter are the best characterized proteases involved in ECM remodeling (9,10), and they have been studied in conditions like inflammation, cancer, arteriosclerosis and fibrosis (11–15). Most MMP are secreted as inactive proform (zymogen) into the extracellular space, where activation is accomplished through cleavage of a propeptide domain (9). Inhibition of MMP occurs by tissue inhibitors of metalloproteases (TIMP) through 1:1 stoichiometric complexion (9). Metzincins, and especially MMP, function as matrix remodeling enzymes. They modulate tissue structure by degradation of collagens, laminins and fibrillin and by cleaving nonstructural ECM proteins such as latent growth factors, adhesion molecules, chemokines or

Table 1: Demographic and clinical characteristics of patients included in microarray analyses

	N[1]	IF/TA I[1]	IF/TA II[1]	IF/TA III[1]
Number of biopsies	7	4	10	8
Age of recipient [years][2]	45 (+16/−13)	46 (+18/−23)	39 (+18/−15)	40 (+19/−15)
Gender of recipient [%male]	86	75	40	100
Age of donor [years][2,3]	44 (+25/−18)	37 (+32/−48)	43 (+18/−26)	51 (+13/−36)
Gender of donor [%male][3]	33	75	43	86
Number of HLA mismatches[2]	1.8 (+2.2/−1.8)	3.3 (+0.8/−1.2)	3.2 (+1.8/−2)	2.5 (+1.5/−2.5)
Time of biopsy [months post tx][2]	25 (+125/−25)	76 (+67/−143)	114 (+104/−70)	72 (+111/−63)
Patients with AR episodes prior to MA-bx	1	1	4	4
Number of patients with CsA-based regimen	6	3	7	2
Number of patients with Tac-based regimen	1	1	3	2
Number of patients with mTor-I-based regimen	0	0	0	2
Serum creatinine [μMol/L][2]	159 (+51/−55)	155 (+112/−45)	213 (+109/−52)	299 (+196/−107)
GFR (MDRD) [mL/min/1.73 m][2]	43 (+20/−18)	45 (+17/−22)	28 (+9/−15)	22 (+10/−17)

[1]Respective patient groups in GEO: NR; CAN I; CAN II; CAN III.
[2]Numbers reflect means and range.
[3]Incomplete initial donor reports in some cases.
CsA = Cyclosporin A; Tac = Tacrolimus; Tx = transplantation; MA-bx = microarray biopsy; mTor-I = mTor inhibitor; GFR = glomerular filtration rate.

cytokines, and thereby activating and or suppressing cell signaling pathways involved in proliferation, angiogenesis, migration and infiltration (10,16). As one example, MMP-7 cleaves E-cadherin, beta4-integrin, decorin, proHB-epidermal growth factor, FasLigand, proTNF-α or plasminogen besides its degradation of fibronectin, collagens I, III-V, laminin or elastin (17).

During IF/TA development in renal allografts, MMP and other metzincins may act as fibrogenic factors via their effect on ECM proteins and signaling pathways (6,9,10,18). Metzincin-related genes include certain transcription factors, activators, substrates or inhibitors, as well as specific cell-surface and cytoplasmic proteins, regulating the function of metzincins (Table S1). Therefore, we investigated expression of metzincins (METS) and of metzincins together with their related genes (MARGS) on mRNA and protein levels utilizing human renal allograft biopsies categorized into Normals (N) and IF/TA grades I, II, III (Banff '05), as well as in IF/TA patient sera.

Materials and Methods

Patients

Biopsies for microarray analyses: Twenty-nine renal allograft biopsies for cause, primarily due to rising serum creatinine ≥10% above baseline, were included in microarray analyses. Patients were enrolled at Services de Néphrologie A and B at Hôpital Tenon, Hôpital Bicetre, Paris and at Hôpital Pellegrin, Bordeaux, France. Demographic and clinical data are provided in Table 1.

About two-thirds of a 16-gauge needle-biopsy was processed for histopathology, the remaining one-third was immediately immersed into RNAlater (Ambion, Austin, TX) for microarray processing. Histological diagnosis was performed by two independent pathologists, and biopsy classification, based on Banff '05 criteria (5), resulted in 7 Normal (N) and 22 IF/TA without evidence of specific etiology. N cases were characterized by unremarkable histology without signs of CNI-toxicity. Respective N patients had low CNI trough levels (mean C_0 <112 ng/mL), and reduced GFR at time of biopsy was explained by functional and not structural impairment, for example, dehydration. Therefore, they served as control group for analyses. The 22 IF/TA cases were graded based on severity of tubulointerstitial features (ci-/ct-score) into IF/TA I (n = 4), IF/TA II (n = 10) and IF/TA III (n = 8).

Only four IF/TA biopsies showed very mild tubular cell injury and/or arteriolar hyalinosis due to CNI treatment, and additional three IF/TA biopsies revealed suspicious signs of CNI-toxicity. In the remaining 15 IF/TA biopsies, signs of CNI-toxicity were not observed. IF/TA III donors were distinctively older than IF/TA I donors, yet their actual biopsies did not reveal major scarring areas.

Immunosuppression at time of biopsy was based on CNI in 25 cases. Cyclosporine A (CsA) was used in 18, tacrolimus (Tac) in 7 cases. The remaining four patients were either treated by an mTor-inhibitor (mTor-I)-based regimen (sirolimus; n = 2) or by corticosteroids with or without azathioprine (Aza; n = 2). CNI and mTor-I treated patients additionally received one or two of the following: corticosteroids, mycophenolate-mofetil or Aza. Trough levels (C_0) of CsA were generally kept between 110 ng/mL and 150 ng/mL, Tac C_0 levels were targeted at 5–10 ng/mL.

Acute T-cell-mediated, biopsy-proven rejection episodes (AR) prior to biopsy for the present study were documented for 10 patients (1 N; 9 IF/TA), dependent on completeness of data. We predominantly found AR I, besides one in each case of AR II and III. Antibody-mediated AR did not occur.

All patients had given written informed consent, and the local ethical commission had approved the study.

Biopsies for microdissection, subsequent qRT-PCR and immunohistochemistry (IHC): For validation and extension of microarray results, 20 archival, formalin fixed-paraffin embedded (FFPE) renal allograft biopsies from our institution were used. Biopsies were classified by two independent pathologists based on Banff '05 (5). Three IF/TA I, 4 IF/TA III and three N biopsies were used for laser capture microdissection (LCM) and subsequent quantitative real time-PCR (qRT-PCR). IHC was performed using

6 IF/TA I, 3 IF/TA II, 6 IF/TA III and 5 N biopsies. Biopsies for LCM and IHC partly originated from the same patients.

Sera for enzyme linked immunosorbent assays (ELISA): For ELISA, we used serum samples of six patients (1 IF/TA I; 5 IF/TA II) from Hôpitals Tenon, Paris and Pellegrin, Bordeaux, France, simultaneously collected to respective microarray-biopsies. Another six serum samples from kidney transplant patients with stable function (GFR > 90 mL/min) (Ctrl-tx) and six from healthy volunteers (Ctrl non-tx) were recruited from our institution serving as age- and sex-matched reference groups.

Preparation of RNA and hybridization of microarrays

RNA was extracted by RNeasy according to the manufacturer's protocol (Qiagen, Hilden, Germany), quantified by ND-1000 spectrophotometer (NanoDrop Technologies, Wilmington, DE) and quality controlled by Bioanalyzer 2100 (Agilent Technologies, Santa Clara, CA). Aliquots of 50 ng total RNA were subjected to Affymetrix 2-cycle cDNA amplification, labeling, and hybridization to Human Genome U133 Plus 2.0 Arrays, containing 54 120 probe sets representing >47 000 different transcripts (Affymetrix, Santa Clara, CA) at the Novartis Genomics Factory in Basel, Switzerland (Affymetrix raw data of biopsies used in our study (Table S2) are available in gene expression omnibus (GEO), microarray data repository GSE9493 (www.ncbi.nlm.nih.gov/geo).

Laser capture microdissection (LCM)

Twelve 5 μm sections per biopsy were mounted onto polyethylene naphthalene (PEN) -membrane covered slides (P.A.L.M., Microlaser Technologies, Bernried, Germany), deparaffinized and stained using hematoxylin. LCM was applied to excise glomeruli, proximal and distal tubules from each section using the P.A.L.M. MicroBeam system (P.A.L.M. Microlaser Technologies). Respective kidney units were highlighted, cut and catapulted into an adhesive tube by a single or several laser shots. All existing glomeruli (16–191), 240–400 proximal and 240–400 distal tubules were captured and collected for each patient. Additionally, we scraped off six sections without glomeruli representing the sample 'tubulointerstitium'. All samples were exposed to Protease K (Arcturus, Bucher Biotec AG, Basel, Switzerland) digestion at 37°C for 20 h before storage at –80°C.

PCR of RNA from microdissected tissues

Total RNA was extracted from microdissected kidney elements and transcribed into cDNA using the Paradise Whole Transcript RT Reagent System (Arcturus, Bucher Biotec AG), and Superscript III RT (Invitrogen AG, Switzerland) was added. All procedures were performed according to the manufacturer's protocols under RNase-free conditions; cDNA samples were stored at –20°C until gene expression analysis.

QRT-PCR was performed using the 7500 Fast Real Time PCR system (Applied Biosystems, Rotkreuz, Switzerland) in Standard 7500 run mode with the following pimers and probes: MMP-7: Hs00159163_m1; MMP-9: Hs00234579_m1; THBS-2: Hs00170248_m1; 18S rRNA (endogenous control): Hs99999901_s1 (Applied Biosystems). Samples were run in triplicates for 40 cycles; a calibrator cDNA sample served as reference value for relative quantification.

Immunohistochemistry (IHC)

IHC for MMP-7 was performed as previously described using 5 μm FFPE sections and an antihuman rat monoclonal MMP-7 antibody (19), diluted 1:100. Staining of fibrillin-1 (mouse monoclonal antihuman FBN-1; c = 4 μg/mL; NeoMarkers, Freemont, CA) using 3 μm FFPE sections was performed as previously published (20). However, for development, a polymer-system consisting of antimouse antibodies and horseradish peroxidase enzymes bound to a dextran backbone (Envision; Dako, Glostrup, Denmark) was applied for 30 min, followed by 0.1% 3,3′-diaminobenzidine and 0.03% H_2O_2 development, counterstaining and mounting.

We scanned the slides using Scan Scope CS System, and Image Scan Scope software v.9.0 was applied for semiquantification (Aperio, Vista, CA). An algorithm counting stain specific positive pixels was used and, in relation to total number of pixels and scanned area, defined as positivity of staining.

ELISA

Quantikine ELISA kits for pro-/active MMP-7, pro-/active MMP-2, THBS-2 and SPP1 from R&D (R&D Systems Europe Ltd, Abingdon, UK) were used according to the manufacturer's protocol. Samples were run in triplicates.

Statistics

Microarrays: Microarray cell intensity (CEL) files were analyzed with Partek Genomics Suite v.6.3 (www.partek.com). Files were subjected to Robust MultiChip Analyses (RMA), quantile normalization with background correction and $\log_2$ transformation. Model-dependent undesired technical processing-related variance was treated by least squared mean adjustment.

For classifier identification, ANOVA and Shrinking Centroids methods were used for variable selection, and a variety of classification methods, such as K-nearest neighbor (KNN) and discriminant analysis (DA) were tested. To limit type 1-error, leave-one-out method was performed for internal cross-validation (21). An internal split into training- and test-set would have resulted in groups with too few samples. The model with the highest specificity/sensitivity was applied to external data sets that were downloaded from public data repositories. The 'Edmonton' data set is found on http://transplants.med.ualberta.ca (22), and the 'Stanford' data set was downloaded from the GEO microarray data repository (GEO343; www.ncbi.nlm.nih.gov/geo) (23). Mapping of Affymetrix probe sets to Stanford array clones of a 'lymphochip' was done by annotation, and missing values were added as median per clone. Only probe sets having expression levels ≥100 in ≥4 samples in our data set were used. Similarly, only clones having data in at least 70% of samples were considered.

Gene set enrichment analysis (GSEA) (www.broad.mit.edu) was applied to detect enriched gene sets in a data set, as described earlier (24).

We estimated the relationship between METS and MARGS and histological Banff ci- and ct-scores based on a previous publication (22). Gene set scores for each IF/TA biopsy were calculated as the mean of fold changes of each probe set relative to the mean expression level of the same probe set in N. METS and MARGS scores were then grouped according to respective ci- or ct-score as the group mean, and 2-tailed p-values were calculated.

PCR and ELISA: QRT-PCR data were analyzed using Sequence Detection Software v.1.4 (Applied Biosystems) and Excel 2005 (Microsoft Office 2000, Microsoft, Redmond, WA). Delta (Δ) Ct values were calculated for all samples. Based on ΔCt values of the internal calibrator sample, gene expression fold changes (fc) were computed for IF/TA I, IF/TA III and N (ΔΔCt method).

Analysis of ELISA was performed in Microsoft Excel 2005.

Significance of differential mRNA expression and protein concentrations in IF/TA was calculated in Graph Pad Prism v.5.01 (Graph Pad Software Inc., LaJolla, CA) applying Mann–Whitney U-test with a p-value < 0.05 as significant. Results are given as mean values plus standard error of mean.

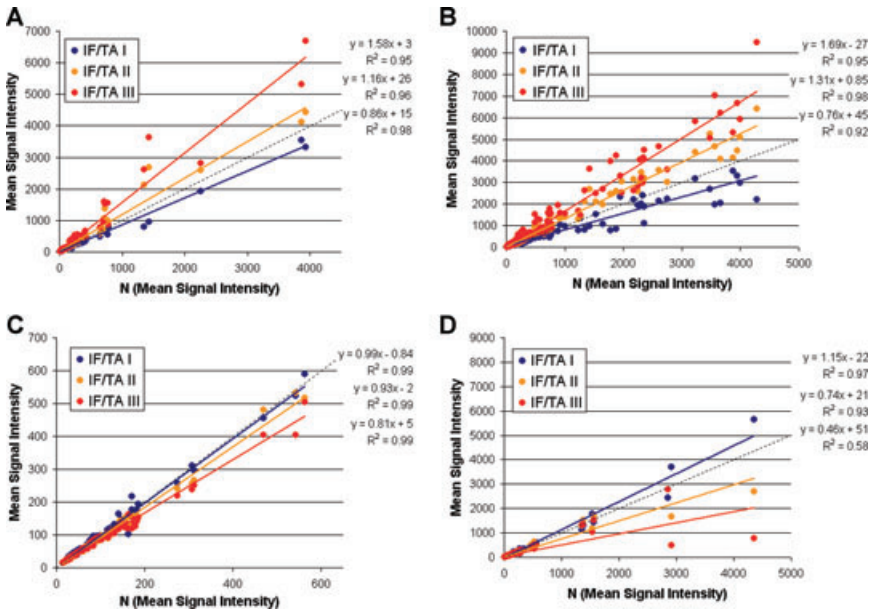

Figure 1: IF/TA grade-dependent expression changes of METS and MARGS. Probe sets with up- (A, B) or downregulation (C, D) in IF/TA compared to N are plotted: on the x-axis mean expression levels of probe sets in N and on the y-axis corresponding expression levels in IF/TA. Each dot represents one probe set. Equations were obtained by linear regression of data points. Slope values >1 reflect overrepresentation and <1 underrepresentation of genes compared to expression in N; exclusion of 4 MARGS probe sets due to probe saturation effects. (A) Upregulated METS (64 probe sets) and (B) upregulated MARGS (213 probe sets) in IF/TA III with respective values for IF/TA II and I. (C) Downregulated METS (93 probe sets) and (D) downregulated MARGS (209 probe sets) in IF/TA III and respective data for IF/TA I and II.

Results

Microarray analysis

We examined expression changes of METS (n = 76) and MARGS (n = 157) (Table S1), in increasing grades of IF/TA.

Among METS, 41% of probe sets, and among MARGS, 50% of probe sets showed increased mean signal intensities with a steady rise from IF/TA I to II and III, as indicated by the increasing slopes of respective regression curves (Figure 1A, B). IF/TA grade-dependent decrease of signal intensities for probe sets having lower than N expression levels in IF/TA III is illustrated in Figure 1C (METS) and 1D (MARGS).

ANOVA was performed with both gene sets on all four sample groups to identify probe sets with significant expression differences explaining the variance between individual sample groups. Five METS probe sets and 12 MARGS probe sets ($p \leq 0.0001$) explained about 66% of the variance between N, IF/TA I, -II, and IF/TA III in the first component of a principal component analysis (PCA) (Figure 2A, B). PCA revealed an IF/TA grade-dependent transition from N to IF/TA II and -III, while IF/TA I samples appeared to be close to N.

To test the potential of METS as molecular markers of IF/TA, we calculated sensitivity, specificity and accuracy of more than 1500 models, using gene expression data of our,

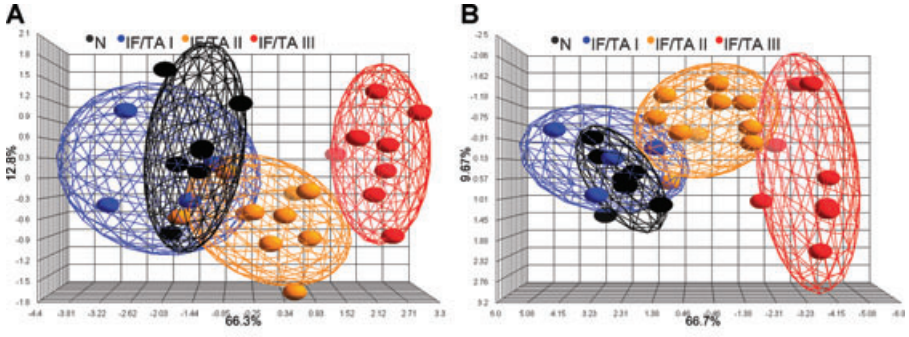

Probeset ID	Gene Symbol	p-value
213532_at	ADAM17	3.61E-06
1569001_at	BMP1	7.24E-06
205745_x_at	ADAM17	4.04E-05
206616_s_at	ADAM22	5.50E-05
214913_at	ADAMTS3	0.000104

Probeset ID	Gene Symbol	p-value
213532_at	ADAM17	3.61E-06
1569001_at	BMP1	7.24E-06
212171_x_at	VEGFA	1.81E-05
210513_s_at	VEGFA	2.75E-05
209977_at	PLG	3.04E-05
210484_s_at	TNFRSF10C	3.94E-05
205745_x_at	ADAM17	4.04E-05
209978_s_at	PLG	4.80E-05
206616_s_at	ADAM22	5.50E-05
211527_x_at	VEGFA	6.46E-05
224374_s_at	EMILIN2	7.73E-05
214913_at	ADAMTS3	0.000104

Figure 2: Principal component analysis (PCA) of ANOVA filtered probe sets illustrates histological IF/TA progression. (A) PCA based on 5 METS probe sets with $p \leq 0.0001$, representing 4 genes. (B) PCA based on 12 MARGS probe sets with $p \leq 0.0001$, representing 8 genes. PCA revealed a trend of IF/TA grade-dependent transition from N to IF/TA III. Probe set lists were generated by ANOVA across all patient groups. The ellipsoids contain data points of the individual groups with a standard deviation of 3.0.

Table 2: Classification performance using a linear discriminant model based on 26 probe sets coding for 20 MARGS

	Correct classification rate [%]	Sensitivity [%]	Specificity [%]
Present study (n = 29)	100	100	100
Edmonton (22) (n = 17)	88	75	100
Stanford (23) (n = 31)	77	67	88

as well as two external, independent data sets: included were 7 N and 22 IF/TA samples of our, 8 N and 9 IF/TA samples of the 'Edmonton' and 15 N and 16 IF/TA samples of the 'Stanford' data set. One model categorized our data set in agreement with histopathological readings and was based on METS. As the accuracy of the external data was insufficient, we repeated analyses applying MARGS. A linear DA with 26 probe sets, including ADAMTSL3, ADAMTS5, ADAM28, THBS-1 and -2 (Table S3), correctly classified all samples in our data set and showed 88% correct assignment of 'Edmonton' (22) (sensitivity 75%, specificity 100%), and 76% correct assignment of 'Stanford' (23) samples (sensitivity 67%, specificity 87%) (Table 2).

To examine possible pathways and molecular processes underlying IF/TA in comparison to normal allografts, we subjected the expression data of IF/TA and N samples to GSEA with 1252 gene sets from various sources. Resulting gene sets contained numerous members of METS or MARGS (Figure 3A–F).

One gene set with enrichment in IF/TA is 'Human Extracellular Matrix and Adhesion Molecules' (ECM; SABioscience Corporation, Frederick, MD) containing MMP, MMP substrates, TIMP, SPP-1, THBS -1,-2,-3 as well as other structural and signaling ECM proteins (Figure 3A).

Similarly, members of the gene set 'epithelial to mesenchymal transition' (EMT; based on (25)) were significantly augmented in IF/TA compared to N (Figure 3B). 'EMT' includes many MMP substrates concerning cell structure, adhesion and signaling. GSEA further associated IF/TA to the winglesstype signaling pathway (Wnt; SABioscience Corporation), including β-catenin (Figure 3D). A potential relation between Wnt-signaling, β-catenin, MMP-7 expression and IF/TA is discussed below. Another gene set illustrating IF/TA involvement is the signaling pathway transforming growth factor-beta (TGF-β) (26) (Figure 3E). On the contrary, members of the gene set 'Aging kidney down' (27), which includes genes with underrepresentation in senescent human renal biopsies, showed enrichment in our N biopsies (Figure 3E) implying that aging related—processes may be involved in IF/TA development.

Next, we focused on the relationship between METS and MARGS and individual Banff scores (ci, ct, cv). Eighteen METS and 89 MARGS probe sets with absolute fc ≥1.5 from N to IF/TA III were included in the analyses. Figure 4 illustrates that increasing expression fc for METS and MARGS relate to rising ci- and ct-scores with significant correlation between ci3 and ci2/ci1 and between ct3 and ct1. No significant correlation was observed for cv scores (data not shown). Generally, METS performed better than MARGS.

Based on the results of microarray analyses and previous studies (28), we selected 17 genes for more detailed investigations. Selection criteria comprised extent of over-/underrepresentation in IF/TA, known involvement in fibrogenesis and ECM remodeling and implication in fibrotic diseases of other organs (10,12,14). Figure 5 illustrates that for most of these genes expression fc (log_2 transformed) to N rose concurrently to IF/TA progression.

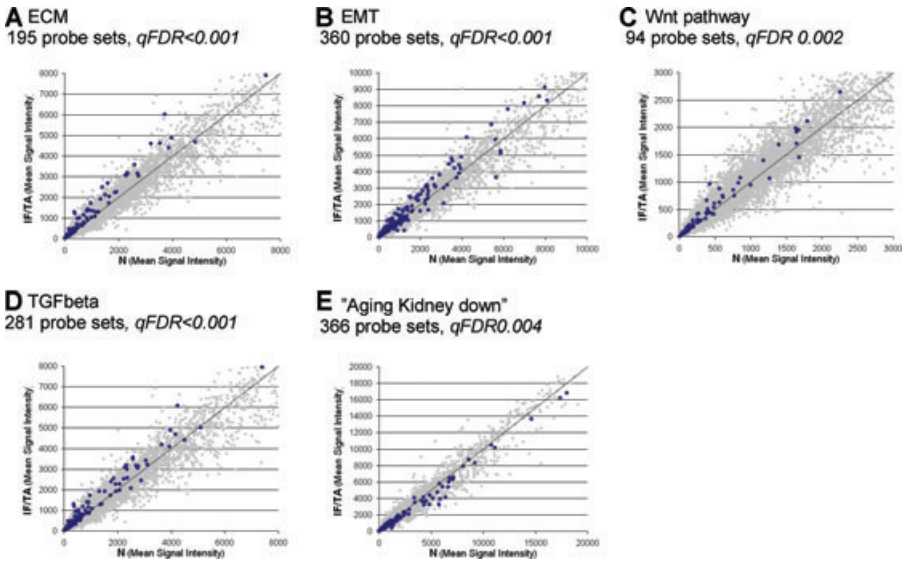

Figure 3: Gene sets reflecting potential pathogenic processes underlying IF/TA are enriched in IF/TA biopsies and include MARGS. GSEA identified pathways and gene sets enriched in IF/TA samples (IF/TA I, II, III combined; n = 22). Mean signal intensities for N (n = 7) and IF/TA are plotted. (A) 'ECM': ECM and adhesion molecules; 195 probe sets (B) 'EMT': 360 probe sets (C) 'Wnt-pathway': 94 probe sets; (D) 'TGFbeta-signaling pathway': 281 probe sets; (E) 'Aging kidney_down', 366 probe sets; genes downregulated in aging kidneys.

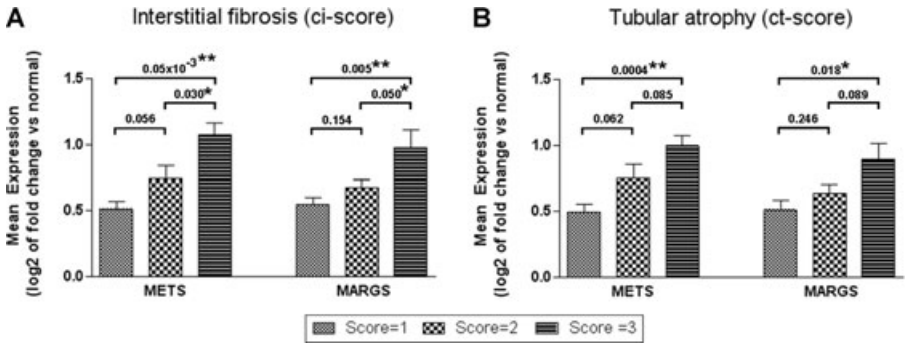

Figure 4: Relationship of METS and MARGS to individual Banff scores. Mean expression levels of individual METS- and MARGS-scores (log2 ± SEM) are plotted for (A) increasing grades of IF (ci1–3) and (B) increasing grades of TA (ct1–3). The p-values were calculated by 2-sided *t*-test. *$p \leq 0.05$; **$p \leq 0.01$.

Highest expression in IF/TA III was observed for MMP-7 and THBS-2 (log2 fc = 1.4; respectively 1.7).

qRT-PCR of RNA from microdissected glomeruli, tubuli and tubulointerstitium

Glomerular, proximal- and distal tubular as well as tubulointerstitial gene expression in N, IF/TA I and IF/TA III were calculated as mean fold change to expression in the internal calibrator sample (Figure 6).

Significant overexpression of MMP-7 (Figure 6A) and THBS-2 (Figure 6B) was observed in all isolated kidney units of IF/TA I and -III biopsies compared to N, except THBS-2 in distal tubules. Both genes showed highest mRNA levels in proximal tubules of IF/TA I biopsies (MMP-7, fc = 26; THBS-2, fc = 33). Glomerular expression of MMP-7 and THBS-2 was low in N, but increased in IF/TA I ($p < 0.05$) –III ($p < 0.001$). Glomerular and tubular expression of MMP-9 were specifically elevated in IF/TA I (data not shown).

Immunohistochemistry

IHC revealed accumulation of MMP-7 and FBN-I in IF/TA I and -III biopsies compared to N (Figure 7). In conformity with qRT-PCR results, protein MMP-7 levels in IF/TA biopsies were more intense in tubules than glomeruli. There were particularly increased MMP-7 levels in distal tubules of IF/TA III (Figure 7C). FBN-I levels were intensified in the interstitium (Figure 7G) and increased from N to IF/TA III confirming microarray findings. Calculated positivity of stainings further supported our observations (Figure 7D, H).

IHC for MMP-2, -9 and TIMP-2 did not lead to identification of a distinct pattern (data not shown).

ELISA of serum samples

Investigations of circulating MMP-2, -7, THBS-2 and SPP-1 levels revealed increased concentrations in IF/TA patients compared to transplanted patients with stable function (Ctrl-tx) or healthy volunteers (Ctrl non-tx) (Figure 8). Differences between IF/TA and control groups were statistically significant in all cases, except THBS-2 versus Ctrl-tx. MMP-7, THBS-2 and SPP-1 progressively rose from Ctrl non-tx to Ctrl tx to IF/TA. Interestingly, Ctrl non-tx already significantly deviated from Ctrl-tx with regard to MMP-2, -7 and SPP-1 (Figure 8A, C, D). Protein levels were more homogenously distributed within the control groups compared to IF/TA.

Additional ELISA for MMP-3/-9 and TGF-β 1 were inconclusive (data not shown).

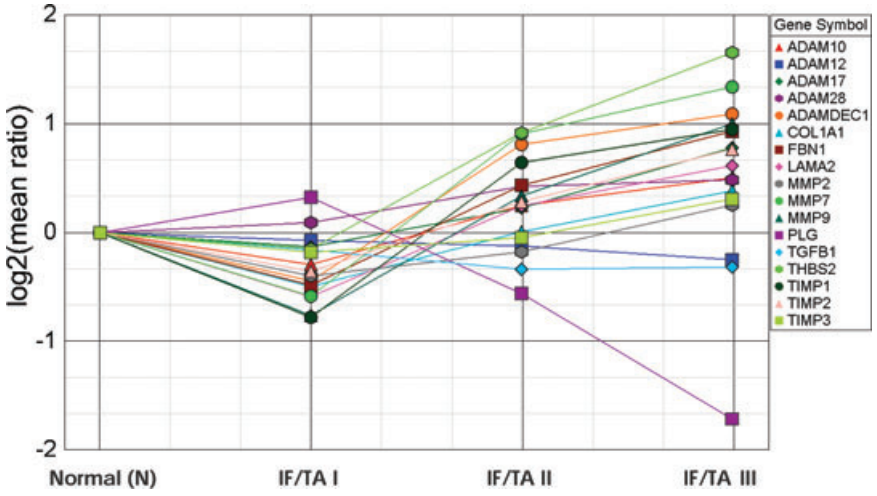

Figure 5: Gene expression changes of 17 MARGS. Relative expression log2 mean ratio to N of selected 32 probe sets monitored by microarray analyses are plotted for three patient groups with increasing IF/TA grade. Mean values were calculated for ADAM12, ADAM17, ADAM28, COL1A1, FBN1, LAMA2, PLG, TIMP2, TIMP3, represented by several probe sets. Log2 values >0 illustrate increased, <0 decreased expression compared to N.

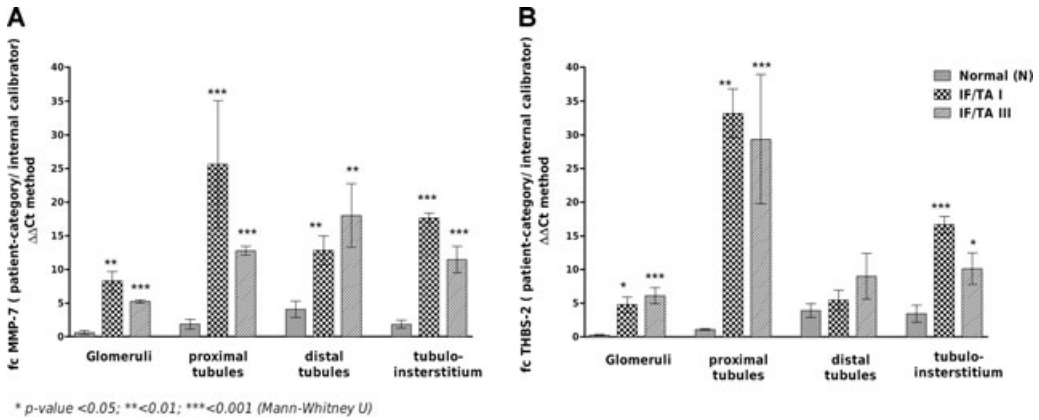

Figure 6: Glomerular and tubular MMP-7 and THBS-2 mRNA levels are augmented in IF/TA I and IF/TA III. Expression of MMP-7 and THBS-2 in microdissected kidney elements of three patient groups (N; IF/TA I; IF/TA III) is illustrated as fc to expression in the internal calibrator sample (A) MMP-7 expression changes in glomeruli, proximal-, distal tubules and tubulointerstitium, (B) respective values for THBS-2. The p-values were calculated by Mann–Whitney U-test; *p ≤ 0.05; **p ≤ 0.01; ***p ≤ 0.001.

Discussion

This study was performed to investigate the role of metzincins and related genes (METS and MARGS) in IF/TA without evidence of specific etiology. Gene and protein expression analyses were performed in independent sets of clinically indicated renal allograft biopsies (biopsies for cause) and in respective patient sera.

To identify differences in expression based on IF/TA development, we chose biopsies histologically classified as 'Normal' (Banff '05) as control group, despite transient functional impairment. Likelihood for normal histology was increased by the low threshold of biopsy indication. Nevertheless, protocol biopsies of recipients with normal allograft function would present an even better control group.

With the help of genechip technology, we identified differences between IF/TA and N based on the expression profiles of METS and MARGS and distinguished deregulated key genes with respect to IF/TA classification and progression.

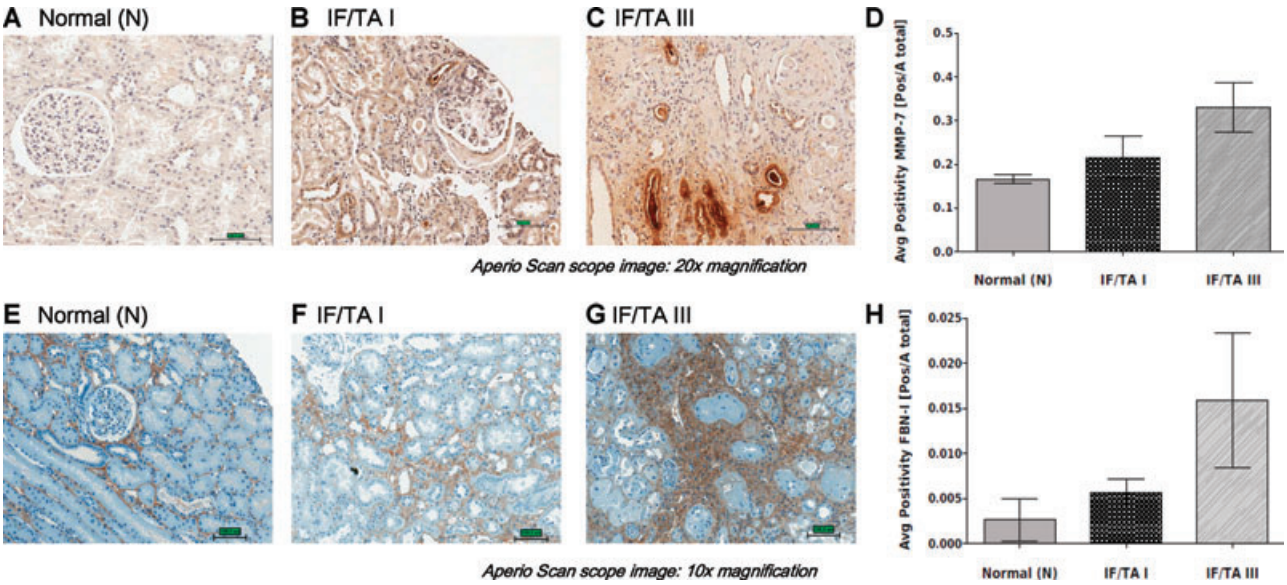

Figure 7: Immunohistology shows increased glomerular and tubular MMP-7 and interstitial FBN-I. MMP-7 and FBN-I IHC of sections from Normal (N), IF/TA I, and IF/TA III. Representative pictures for MMP-7 are shown in (A) Normal (N); (B) IF/TA I; (C) IF/TA III biopsies and (D) semiquantification of MMP-7 staining intensity. (E–H) with respective results for FBN-I IHC.

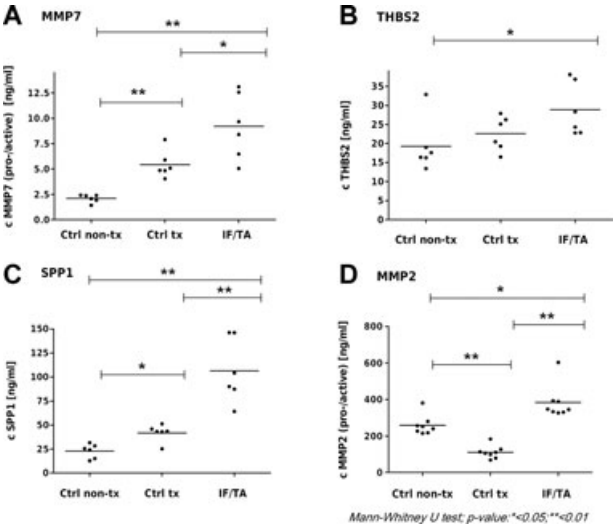

Figure 8: Identification of augmented MMP-7, THBS-2, SPP1 and MMP-2 serum levels. ELISA demonstrated elevated concentrations of MMP-7, MMP-2, THBS-2 and SPP1 in the circulation of patients with IF/TA I, II. Each dot represents one sample, and the lines represent mean serum levels.

Our analyses focused on metzincins due to their biological function as ECM-degrading enzymes and their role in activation and suppression of cell signaling pathways with regard to tissue remodeling (9,18). MMP are known to be deregulated in fibrogenic processes, for example, pulmonary, liver and heart fibrosis as well as during progressive kidney scarring (11–14). We previously showed a significant increase of several METS, including MMP, TIMP and ADAM in the established Fisher (F344) to Lewis (LEW) rat model of chronic renal allograft rejection (28).

Little is known about the role of MMPs, metzincins and related genes in human IF/TA. A deregulation of METS and MARGS on mRNA and protein level may indeed contribute to the pathogenesis of IF/TA with respect to their role in fibrosis.

Excessive ECM deposition can be accelerated by EMT, and transition of tubular epithelial to mesenchymal cells has been linked to kidney fibrosis (29,30). IF/TA biopsies of our study showed enrichment of EMT-related genes including metzincins and related genes. Alterations in the cellular composition of tissue, for example, the kidney, including an increase of mesenchymal cells may lead to modulated metzincin expression (17,31,32).

Wnt-signaling can induce EMT and may be involved in renal fibrosis (15,33–36). One target gene of Wnt-signaling is MMP-7 with β-catenin promoting its expression (37). IF/TA biopsies of our study revealed Wnt-signaling involvement, and we observed increasing β-catenin levels during IF/TA progression (data not shown). One consequence of activated Wnt-/ β-catenin signaling may be overexpression of MMP-7, as we observed in IF/TA biopsies. Overexpression of β-catenin in chondrocytes led to increased expression of MMP-7 (38). Our results of tubulointerstitial MMP-7 overexpression in IF/TA agree with findings of others (39,40). In addition, we identified glomerular MMP-7 levels to be increased early during IF/TA, and a preferential distal tubular expression of MMP-7 during progression of IF/TA that was confirmed on the protein level. Furthermore, we discovered elevated MMP-7 levels in IF/TA patient sera.

Elevated mRNA and protein levels in IF/TA patient biopsies and sera were also found for THBS-2. Analyses showed a positive proportionality between increasing THBS-2 mRNA expression levels and IF/TA progression from N to IF/TA I, -II, -III, together with an inverse proportionality to GFR of IF/TA patients (data not shown).

Importantly, our second patient set revealed upregulated mRNA levels of MMP-7 and THBS-2 and increased MMP-7 production already in IF/TA I.

To the best of our knowledge, involvement of THBS-2 in IF/TA has not been reported so far. Others identified THBS-1 as profibrotic factor in IF/TA (40). We saw a twofold augmentation of THBS-1 in the IF/TA patients of our cohort. Since the respective value for THBS-2 was threefold, we further investigated THBS-2. Increase of THBS-2 may lead to decrease of MMP activity, possibly through direct binding (41). Investigating MMP-2, we found insignificant changes in biopsies, however, IF/TA patient sera displayed elevated levels.

Another molecule with overexpression on mRNA and on protein level in IF/TA was SPP-1 that modulates fibroblast secretion of MMP (42–44). Others identified SPP-1 overexpression and an interaction with MMP-7 in patients with pulmonary fibrosis (45).

Of interest is also the increase of FBN-I, detected on mRNA and protein level in IF/TA. FBN-I represents a potential substrate of MMP-7 (46). Predominantly, MMP-7 was found in tubules whereas FBN-I was present in the interstitium.

The findings of our study support a pathogenic role of MMP and their regulators in IF/TA, possibly even indicating novel therapeutic targets for IF/TA treatment. Interventional studies need to validate these findings and may consist of selective MMP (e.g. MMP-7) inhibition. In a mouse model of cardiac rejection, broad systemic MMP- and ADAM-inhibition by doxycycline significantly enhanced allograft survival (47). Doxycycline can indeed inhibit MMP-7 activity (48). Furthermore, early MMP-inhibition by BAY12–9566 resulted in reduced proteinuria associated with an amelioration of IF/TA in rats (49). Sirolimus ameliorated enhanced MMP-2/–9 expression in a rat model of autosomal polycystic disease (50).

The potential of METS and MARGS to complement identification of IF/TA and to indicate progression from N to IF/TA III was supported by the correlation between METS/MARGS and the IF/TA relevant Banff scores ci and ct; there was no correlation with cv scores.

These findings together with linear DA and PCA results for METS and MARGS may be useful to define IF/TA based on genechip technology.

We acknowledge, that our study was primarily limited by a relative small sample size. Microarray data validation in two external data sets and performance of multiple expression analyses using two independent patient populations increased the explanatory power of our analyses and addressed the limiting number of patients. Another limiting factor was the discrepancy between IF/TA I and III patients with respect to donor age. The effect of donor age on our study is difficult to assess due to the small data set, the lack of an independent validation set and the absence of implant biopsies.

Based on our present findings, we conclude, that deregulation of METS and MARGS in IF/TA, especially MMP-7, is able to reflect disease progression and to differentiate this disorder from normal tissue. Patient monitoring applying a transcript-set including these genes might support identification of IF/TA in patients after renal transplantation.

Acknowledgments

We thank Agence de Biomedecine, France; Genomics Factory, Novartis Pharma AG, M. Körner and A. Kappeler from the Institute of Pathology, University Bern, Switzerland and H. Crawford from Stony Brook University, New York, USA for their contributions to this work. Funding sources: Swiss National Science Foundation (NFP-46); INSERM, Unite 702, Hôpital Tenon, Paris, France.

References

1. Solez K, Colvin RB, Racusen LC et al. Banff 07 classification of renal allograft pathology: Updates and future directions. Am J Transplant 2008; 8: 753–760.
2. Halloran PF, Melk A, Barth C. Rethinking chronic allograft nephropathy: The concept of accelerated senescence. J Am Soc Nephrol 1999; 10: 167–181.
3. Nankivell BJ, Borrows RJ, Fung CL, O'Connell PJ, Allen RD, Chapman JR. The natural history of chronic allograft nephropathy. N Eng J Med 2003; 349: 2326–2333.
4. Joosten SA, Sijpkens YW, van Kooten C, Paul LC. Chronic renal allograft rejection: Pathophysiologic considerations. Kidney Int 2005; 68: 1–13.
5. Solez K, Colvin RB, Racusen LC et al. Banff '05 Meeting Report: Differential diagnosis of chronic allograft injury and elimination of chronic allograft nephropathy ('CAN'). Am J Transplant 2007; 7: 518–526.
6. Zeisberg M, Soubasakos MA, Kalluri R. Animal models of renal fibrosis. Methods Mol Med 2005; 117: 261–272.
7. Giannelli G, Quaranta V, Antonaci S. Tissue remodelling in liver diseases. Histol Histopathol 2003; 18: 1267–1274.
8. Nagase H, Woessner JF Jr. Matrix metalloproteinases. J Biol Chem 1999; 274: 21491–21494.
9. Woessner JF Jr. Matrix metalloproteinases and their inhibitors in connective tissue remodeling. Faseb J 1991; 5: 2145–2154.
10. Stamenkovic I. Extracellular matrix remodelling: The role of matrix metalloproteinases. J Pathol 2003; 200: 448–464.
11. Ahmed AK, Haylor JL, El Nahas AM, Johnson TS. Localization of matrix metalloproteinases and their inhibitors in experimental progressive kidney scarring. Kidney Int 2007; 71: 755–763.
12. Huang CC, Chuang JH, Chou MH et al. Matrilysin (MMP-7) is a major matrix metalloproteinase upregulated in biliary atresia-associated liver fibrosis. Mod Pathol 2005; 18: 941–950.
13. Boixel C, Fontaine V, Rucker-Martin C et al. Fibrosis of the left atria during progression of heart failure is associated with increased matrix metalloproteinases in the rat. J Am Coll Cardiol 2003; 42: 336–344.
14. Pardo A, Gibson K, Cisneros J et al. Up-regulation and profibrotic role of osteopontin in human idiopathic pulmonary fibrosis. PLoS Medicine 2005; 2: e251.
15. Shackel NA, McGuinness PH, Abbott CA, Gorrell MD, McCaughan GW. Insights into the pathobiology of hepatitis C virus-associated cirrhosis: Analysis of intrahepatic differential gene expression. Am J Pathol 2002; 160: 641–654.
16. Bergers G, Coussens LM. Extrinsic regulators of epithelial tumor progression: Metalloproteinases. Curr Opin Genet Dev 2000; 10: 120–127.
17. Wilson CL, Matrisian LM. Matrilysin: An epithelial matrix metalloproteinase with potentially novel functions. Int J Biochem Cell Biol 1996; 28: 123–136.
18. Streuli C. Extracellular matrix remodelling and cellular differentiation. Curr Opin Cell Biol 1999; 11: 634–640.
19. Fingleton B, Powell WC, Crawford HC, Couchman JR, Matrisian LM. A rat monoclonal antibody that recognizes pro- and active MMP-7 indicates polarized expression in vivo. Hybridoma (2005) 2007; 26: 22–27.
20. Lods N, Ferrari P, Frey FJ et al. Angiotensin-converting enzyme inhibition but not angiotensin II receptor blockade regulates matrix metalloproteinase activity in patients with glomerulonephritis. J Am Soc Nephrol 2003; 14: 2861–2872.
21. Fan L, Wang S, Wang H, Guo T. Singular points detection based on zero-pole model in fingerprint images. IEEE Trans Pattern Analysis Machine Intelligence 2008; 30: 929–940.
22. Mueller TF, Einecke G, Reeve J et al. Microarray analysis of rejection in human kidney transplants using pathogenesis-based transcript sets. Am J Transplant 2007; 7: 2712–2722.
23. Alizadeh A, Eisen M, Davis RE et al. The lymphochip: A specialized cDNA microarray for the genomic-scale analysis of gene expression in normal and malignant lymphocytes. Cold Spring Harb Symp Quant Biol 1999; 64: 71–78.
24. Subramanian A, Kuehn H, Gould J, Tamayo P, Mesirov JP. GSEA-P: A desktop application for Gene Set Enrichment Analysis. Bioinformatics (Oxford, UK) 2007; 23: 3251–3253.
25. Jechlinger M, Grunert S, Tamir IH et al. Expression profiling of epithelial plasticity in tumor progression. Oncogene 2003; 22: 7155–7169.
26. Branton MH, Kopp JB. TGF-beta and fibrosis. Microbes and infection/Institut Pasteur 1999; 1: 1349–1365.
27. Rodwell GE, Sonu R, Zahn JM et al. A transcriptional profile of aging in the human kidney. PLoS Biol 2004; 2: e427.
28. Berthier CC, Lods N, Joosten SA et al. Differential regulation of metzincins in experimental chronic renal allograft rejection:

Potential markers and novel therapeutic targets. Kidney Int 2006; 69: 358–368.
29. Kalluri R, Neilson EG. Epithelial-mesenchymal transition and its implications for fibrosis. J Clin Invest 2003; 112: 1776–1784.
30. Zeisberg M, Bonner G, Maeshima Y et al. Renal fibrosis: Collagen composition and assembly regulates epithelial-mesenchymal transdifferentiation. Am J Pathol 2001; 159: 1313–1321.
31. Unemori EN, Werb Z. Reorganization of polymerized actin: A possible trigger for induction of procollagenase in fibroblasts cultured in and on collagen gels. J Cell Biol 1986; 103: 1021–1031.
32. Tremble PM, Lane TF, Sage EH, Werb Z. SPARC, a secreted protein associated with morphogenesis and tissue remodeling, induces expression of metalloproteinases in fibroblasts through a novel extracellular matrix-dependent pathway. J Cell Biol 1993; 121: 1433–1444.
33. Wu Y, Zhou BP. New insights of epithelial-mesenchymal transition in cancer metastasis. Acta Biochimica et Biophysica Sinica 2008; 40: 643–650.
34. Surendran K, McCaul SP, Simon TC. A role for Wnt-4 in renal fibrosis. Am J Physiol 2002; 282: F431–441.
35. Chilosi M, Poletti V, Zamo A et al. Aberrant Wnt/beta-catenin pathway activation in idiopathic pulmonary fibrosis. Am J Pathol 2003; 162: 1495–1502.
36. Clevers H. Wnt/beta-catenin signaling in development and disease. Cell 2006; 127: 469–480.
37. Brabletz T, Jung A, Dag S, Hlubek F, Kirchner T. Beta-catenin regulates the expression of the matrix metalloproteinase-7 in human colorectal cancer. Am J Pathol 1999; 155: 1033–1038.
38. Tamamura Y, Otani T, Kanatani N et al. Developmental regulation of Wnt/beta-catenin signals is required for growth plate assembly, cartilage integrity, and endochondral ossification. J Bioll Chem 2005; 280: 19185–19195.
39. Flechner SM, Kurian SM, Solez K et al. De novo kidney transplantation without use of calcineurin inhibitors preserves renal structure and function at two years. Am J Transplant 2004; 4: 1776–1785.
40. Hotchkiss H, Chu TT, Hancock WW et al. Differential expression of profibrotic and growth factors in chronic allograft nephropathy. Transplantation 2006; 81: 342–349.
41. Yang Z, Strickland DK, Bornstein P. Extracellular matrix metalloproteinase 2 levels are regulated by the low density lipoprotein-related scavenger receptor and thrombospondin 2. J Biol Chem 2001; 276: 8403–8408.
42. Schroen B, Heymans S, Sharma U et al. Thrombospondin-2 is essential for myocardial matrix integrity: Increased expression identifies failure-prone cardiac hypertrophy. Circ Res 2004; 95: 515–522.
43. Spinale FG. Cell-matrix signaling and thrombospondin: Another link to myocardial matrix remodeling. Circ Res 2004; 95: 446–448.
44. Bornstein P, Agah A, Kyriakides TR. The role of thrombospondins 1 and 2 in the regulation of cell-matrix interactions, collagen fibril formation, and the response to injury. Int J Biochem Cell Biol 2004; 36: 1115–1125.
45. Mazzali M, Kipari T, Ophascharoensuk V, Wesson JA, Johnson R, Hughes J. Osteopontin–a molecule for all seasons. Qjm 2002; 95: 3–13.
46. Changotade SI, Assoumou A, Gueniche F et al. Epigallocatechin gallate's protective effect against MMP7 in recessive dystrophic epidermolysis bullosa patients. J Investig Dermatol 2007; 127: 821–828.
47. Eaton VL, Lerret NM, Velasquez-Lopera MM et al. Enhanced allograft survival and modulation of T-cell alloreactivity induced by inhibition of MMP/ADAM enzymatic activity. Am J Transplant 2008; 8: 507–516.
48. Garcia RA, Pantazatos DP, Gessner CR, Go KV, Woods VL Jr., Villarreal FJ. Molecular interactions between matrilysin and the matrix metalloproteinase inhibitor doxycycline investigated by deuterium exchange mass spectrometry. Mol Pharmacol 2005; 67: 1128–1136.
49. Lutz J, Yao Y, Song E et al. Inhibition of matrix metalloproteinases during chronic allograft nephropathy in rats. Transplantation 2005; 79: 655–661.
50. Berthier CC, Wahl PR, Le Hir M et al. Sirolimus ameliorates the enhanced expression of metalloproteinases in a rat model of autosomal dominant polycystic kidney disease. Nephrol Dial Transplant 2008; 23: 880–889.

Supporting Information

Additional Supporting Information may be found in the online version of this article:

Table S1: Genechip IDs of biopsies used for present analyses.

Table S2: Description of gene-sets used for microarray analyses.

Table S3: List of 20 MARGS identified by classification performance.

Please note: Wiley-Blackwell is not responsible for the content or functionality of any supporting materials supplied by the authors. Any queries (other than missing material) should be directed to the corresponding author for the article.